Pharm Res (2015) 32:3593–3603
DOI 10.1007/s11095-015-1633-2

RESEARCH PAPER

Evaluation of Targets for Maytansinoid ADC Therapy Using a Novel Radiochemical Assay

Katharine C. Lai • Jutta Deckert • Yulius Y. Setiady • Prerak Shah • Lintao Wang • Ravi Chari • John M. Lambert

Received: 20 October 2014 / Accepted: 16 January 2015 / Published online: 29 January 2015

ABSTRACT

Purpose Many antibody-drug conjugates (ADCs) become active only after antigen-mediated internalization and release of the cytotoxic agent *via* antibody degradation. Quantifying these processes can provide critical information on the suitability of a particular receptor target or antibody for ADC therapy by providing insight into the amount of cytotoxic agent released. We describe a simple and inexpensive radiolabel assay to monitor this process in cultured cancer cells.

Methods Monoclonal antibodies were trace-labeled at their lysine residues by treatment with the *N*-hydroxysuccinimide ester of [^{3}H]propionic acid. Human cancer cell cultures were treated with the labeled antibody at concentrations sufficient to saturate the targeted antigen. After washing to remove unbound antibody, cells were incubated and analyzed for antigen expression, conjugate degradation and catabolite formation. Results were compared with data obtained from similar assays run with radiolabeled antibody-[^{3}H]maytansinoid conjugates ([^{3}H]AMCs). To exemplify the method, studies were conducted with a panel of [^{3}H]propionamide-antibodies to evaluate processing efficiency in EGFR-expressing SCCHN cell lines, and in NHL cell lines expressing the B-cell targets CD19, CD20, CD22 and CD37.

Results Use of the [^{3}H]propionamide-antibody assay yielded cell-mediated processing results similar to those obtained with corresponding maytansinoid ADCs. Further exploration allowed comparison of expression levels, antigen-dependent degradation, and catabolite formation across a panel of EGFR-expressing SCCHN cell lines, and for multiple targets in various B-cell cancer indications.

Conclusions The [^{3}H]propionamide-antibody assay described here is a sensitive, facile method which enables rapid and robust assessment of relative antibody processing amounts for target, antibody, and cell line evaluation.

K. C. Lai (✉) • J. Deckert • Y. Y. Setiady • P. Shah • L. Wang • R. Chari • J. M. Lambert
ImmunoGen, Inc., Waltham, Massachusetts, USA
e-mail: Kate.Lai@immunogen.com

KEY WORDS ADC · antibody-drug conjugate · antigen-mediated delivery · maytansine

ABBREVIATIONS

[^{3}H]Ab	Antibody labeled at lysine residues by treatment with *N*-succinimidyl-[2,3-^{3}H] propionate
[^{3}H]AMC	Ab-SMCC-[^{3}H]DM1 with tritium incorporated on the C20 methoxy group of DM1
Ab	Antibody
ABC	Antibody bound per cell
ADC	Antibody drug conjugate
AMC	Antibody maytansinoid conjugate
Ci	Curie
CPM	Counts per minute
DLBCL	Diffuse large B-cell lymphoma
DM1	L-DM1, the name for $N^{2'}$-deacetyl-$N^{2'}$-(3-mercapto-1-oxopropyl)-maytansine
DM4	L-DM4, the name for $N^{2'}$-deacetyl-$N^{2'}$-(4-mercapto-4-methyl-1-oxopentyl)-maytansine
DPM	Disintegrations per minute
FBS	Fetal bovine serum
HILIC	Hydrophilic interaction liquid chromatography
J2898A	Anti-EGFR antibody
LC/MS	Liquid chromatography followed by Mass spectrometry
LSC	Liquid scintillation counting
Na_2EDTA	Ethylenediaminetetraacetic acid, disodium salt
NHL	Non-Hodgkin lymphoma
PBS	Phosphate-buffered saline, pH 7.4
SCCHN	Squamous cell carcinoma of the head and neck
SMCC	Succinimidyl-4-(*N*-maleimidomethyl) cyclohexane-1-carboxylate
T-DM1	Ado-trastuzumab emtansine
UV/Vis	Ultra-violet/visible range spectroscopy

INTRODUCTION

Antibody-drug conjugates (ADCs) containing a maytansinoid cytotoxic agent (AMCs), have demonstrated remarkable *in vivo* anti-tumor activity with antibodies to a wide range of targets expressed on many different cancers in preclinical studies. AMCs have also shown clinically-proven anti-tumor activity at doses that exhibit good tolerability (1). Ado-trastuzumab emtansine (Kadcyla®, T-DM1), an AMC comprising the HER2-targeting trastuzumab antibody linked to maytansinoid DM1 *via* non-cleavable SMCC linkage, was FDA-approved in February 2013 for its first indication, the first ADC to receive full approval based on a randomized Phase 3 study. In addition to T-DM1, several other AMCs have shown promising signals of clinical efficacy and good tolerability in early-phase clinical trials (1–5).

The mechanism of action and metabolic fate of AMCs upon delivery to cancer cells has been well documented (6–9). Studies using ADCs made with radiolabeled maytansinoids, [^{3}H]DM1 and [^{3}H]DM4, enabled determination of their biodistribution and pharmacokinetic properties as well as the identification of catabolites derived from AMCs. Upon cellular uptake *via* target-mediated endocytosis, the antibody portion of an AMC is degraded in the lysosome, yielding catabolites consisting of the lysine-linker-maytansinoid (6). For ADCs with a thioether linkage, such as T-DM1, lysine-SMCC-DM1 is the sole catabolite. For conjugates with a disulfide linkage, such as the CD19-targeting coltuximab ravtansine (SAR3419), the lysine-linker-maytansinoid catabolite can undergo disulfide reduction and subsequent *S*-methylation of the maytansinoid thiol to yield additional intracellular products (6,10). All maytansinoid catabolites are able to bind to tubulin present in mitotic spindles, arresting cells in G2/M phase, and eventually causing cell death (6,7).

Studies utilizing AMCs in which the maytansinoid molecule is radiolabeled are highly informative, since the quantity of catabolites generated from lysosomal processing of the actual therapeutic candidate molecule are directly measured (6–8,11–14). This is in contrast to traditional methods of studying receptor trafficking, such as biotinylation, which measures only the constitutive receptor recycling, or the use of fluorescent antibodies which are difficult to quantify (15,16). However, the use of radiolabeled maytansinoid is not practical for many projects, particularly those in early discovery, due to the need to conduct specialized radiolabeled synthesis of the maytansinoid payload and cumbersome preparation and purification of each radiolabeled ADC. In order to obtain information about the suitability of a target without requiring [^{3}H]DM1 or [^{3}H]DM4 conjugates we have developed a highly sensitive assay to probe target-mediated lysosomal degradation and catabolite formation, allowing exploration of numerous targets and cell lines. We trace-labeled antibodies at their lysine residues with a commercially available radiolabeling agent that has high specific radioactivity (*N*-succinimidyl-[2,3-^{3}H] propionate) to form [^{3}H] propionamide-labeled antibodies ([^{3}H]Abs), as an alternative to the established [^{3}H]AMC procedures. The [^{3}H]Ab assay enabled use of small *in vitro* samples to assess the level of antigen, target-mediated degradation and quantification of catabolite simultaneously in a rapid and robust manner which orthogonal non-radioactive methods could not match without increased sample number, size and/or confounding matrix effects.

Before testing extensive panels of cell lines and targets we evaluated the methods to ensure that the [^{3}H]Ab reagent and corresponding [^{3}H]AMC gave similar results for antigen expression, extent of conjugate degradation and catabolite formation. Using the [^{3}H]Ab assay to screen multiple B-cell targets on several cell lines, we obtained comparable target information quickly while eliminating the need for specialized reagent synthesis, aiding greatly in rapidly screening targets and selecting lead antibodies suitable for an ADC application.

MATERIALS AND METHODS

Materials

The following cell lines were obtained from American Type Culture Collection (ATCC, Manassas, VA): A253, H1975, H292, Detroit 562, FaDu, SCC4, SCC9, Ramos, Daudi, Raji, and Farage. The following cell lines were obtained from Japanese Collection of Research Bioresources (JCRB) Cell Bank (Osaka, Japan): CA922, HSC-2, OSC-19 and SAS. The following cell lines were obtained from German Collection of Microorganisms and Cell Cultures (DSMZ; Braunschweig, Germany): CAL33 and SU-DHL-4. BJAB cells were obtained from Elliot Kieff (Harvard University Medical School). Cells were grown at 37°C in a humidified 5% CO_2 incubator and passaged by diluting into fresh media supplemented with 10% FBS 2–3 times per week to maintain a cell density between 0.2 and 2×10^6 cells/ml.

Tissue culture plates and polypropylene tubes were obtained from Corning Incorporated, Corning, NY. Phosphate-buffered saline (PBS) was from Invitrogen, Carlsbad, CA. *N*-succinimidyl-[2,3-^{3}H]propionate in ethyl acetate (80 Ci/mmol) was from American Radiolabeled Chemicals, St. Louis, MO. The monoclonal anti-CD20 antibody rituximab (Rituxan®) was obtained from a commercial source (RxUSA Wholesale Inc., Port Washington, NY). The humanized monoclonal antibodies against CD19 (huB4), CD22 (huBU59), CD37 (K7153A) and EGFR (J2898A) were prepared in-house (ImmunoGen, Inc.,

Waltham, MA). Solvable™ protein solubilizer, Ultima Gold scintillation fluid, and scintillation vials were from PerkinElmer, Waltham, MA. Amicon centrifugation concentration units were from Millipore, Billerica, MA. Illustra Sephadex G-25 columns were from GE Healthcare, Pittsburg, PA.

Conjugate Generation

Humanized monoclonal antibodies were labeled at lysine residues by treatment with *N*-succinimidyl-[2,3-^{3}H]propionate (#0135, ARC, Inc.) to provide [^{3}H]propionamide-antibodies ([^{3}H]Abs) with a specific radioactivity of ~25 Ci/mmol (see Fig. 1a). Aliquots (0.5–1 mCi) of the tritiated reagent in ethyl acetate were dried down in 1 ml glass vials under nitrogen. The dried *N*-succinimidyl-[2,3-^{3}H]propionate was dissolved in 0.67 ml of 100 mM HEPES, pH 8, containing 2 mg of antibody and incubated for 90 min at room temperature. Unreacted radiolabeled reagent was separated from modified antibody using a centrifugal concentration unit (Amicon UFC 500324, Millipore). Samples were concentrated to about 0.2 ml and diluted with PBS to about 1 ml in the centrifugal units for repeat cycles of centrifugation until minimal radioactivity was detected in the eluent (5–8 cycles). Final conjugates were assayed for concentration of antibody by UV/Vis spectrometry and for [^{3}H] incorporation by liquid scintillation counting (LSC) to determine the specific radioactivity.

Radiolabeled EGFR-targeting ADC (J2898A-SMCC-[^{3}H]DM1) was prepared by modifying the J2898A antibody *via* lysine residues with a premade solution of SMCC-DM1 formed by reacting *N*-succinimidyl 4-(N-maleimidomethyl) cyclohexane-1-carboxylate (SMCC) with a 1.3-fold molar excess of $N^{2'}$-deacetyl-$N^{2'}$-(3-mercapto-1-oxopropyl)-maytansine (DM1) bearing a tritium label at its C-20-methoxy group. The tritium-labeled DM1 was prepared from ansamitocin P-3 as previously described (17): briefly, the C20 methoxy group of ansamitocin P-3 was demethylated by incubation with the bacterial strain *Streptomyces platensis* to give ansamitocin PDM-3 (18), and then the C-20-OH moiety of ansamitocin PDM-3 was methylated using [^{3}H]CH_3I by a method described by Sawada (19). The J2898A-SMCC-[^{3}H]DM1 conjugation mixture was incubated overnight at room temperature prior to gel filtration on a Sephadex G25 column. The purified conjugate was analyzed for concentration of antibody and DM1 by UV/Vis spectrometry and for [^{3}H] incorporation by LSC to determine the specific radioactivity. To determine the amount of tritium radioactivity that was not bound to protein in each antibody or conjugate preparation ([^{3}H]$_{free}$), samples of purified [^{3}H]Ab and [^{3}H]AMC were extracted with ice-cold acetone (4:3 acetone: aqueous sample) and frozen for a minimum of 1 h at -80°C. The samples were spun down and the supernate was counted by LSC. The amount of [^{3}H]$_{free}$ was determined by calculating the radioactivity

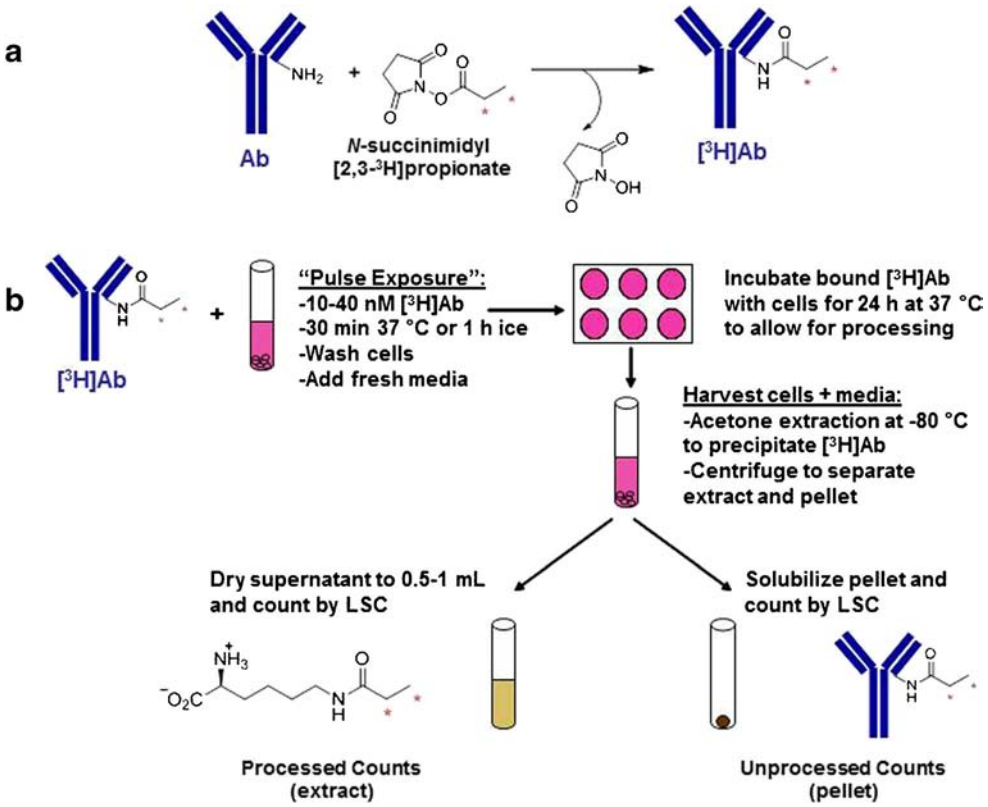

Fig. 1 Ab labeling with *N*-succinimidyl-[2,3-^{3}H]propionate and *in vitro* processing method. Reaction scheme displaying Ab labeling with *N*-succinimidyl-[2,3-^{3}H]propionate. The tritium label is indicated by red asterisks (**a**). The *in vitro* processing method separates unprocessed counts (protein-containing pellet) and processed counts (soluble acetone extract) (**b**).

of the supernate/radioactivity for Ab or conjugate (see above) × 100%.

Pulse Treatment of Cells with [^{3}H]Ab or [^{3}H]AMC

Cultures of cells in media ($1-2\times10^6$ per ml) supplemented with 10% FBS were exposed to 10–40 nM of [^{3}H]Ab or [^{3}H]AMC for 30 min at 37°C or 1 h on ice. Cells were washed three times in media to remove any unbound conjugate, re-suspended in fresh culture medium and incubated at 37°C with 5% CO_2 for the amount of time specified.

After the indicated time at 37°C, [^{3}H]Ab-treated cells and media were harvested and extracted with acetone (4 volumes per 3 volumes of sample) in order to separate soluble [^{3}H]-labeled species from protein-associated species. Samples were frozen at -80°C for a minimum of 1 h to fully precipitate the protein. Samples were thawed and centrifuged at 2,000×*g* for 15 min and supernatants and the protein-containing pellets were separated. The supernates containing the protein-free catabolites (also referred to as the 'extract') were evaporated to dryness using an evacuated centrifuge and the residue was resuspended in PBS (0.5 ml) and Ultima Gold scintillation cocktail (4 ml) and counted for 5 min in a Tri-Carb 2900 T liquid scintillation counter. The acetone pellets containing precipitated [^{3}H]Ab were re-suspended in water (0.3 ml), dissolved by the addition of 1 mL Solvable^{TM} reagent and incubated overnight in a 50°C water bath. Samples were removed from incubation and 0.1 ml of 0.1 M Na_2EDTA and 0.3 ml of 30% hydrogen peroxide were added to each sample followed by 15 min incubation at room temperature. Samples were then incubated for 1 h at 50°C before addition of 0.25 ml of 1 N HCl and 15 ml Ultima Gold scintillation fluid. Samples were agitated vigorously and kept in the dark for a minimum of 4 h to minimize background luminosity before counting by LSC. See Fig. 1b.

For the identification of the cellular degradation products, evaporated extract was resuspended in 20% 50 mM acetic acid/80% acetonitrile (by volume) and separated by HPLC using a HILIC column (SeQuant ZIC-HILIC, 150×4.6 mm) heated to 25°C and eluting with a gradient of decreasing acetonitrile over 30 min. The effluent was collected in 1 ml fractions and the radioactivity associated with each fraction was determined by mixing each vial with Ultima Gold liquid scintillation cocktail (4 ml) before counting by LSC.

Cells treated with [^{3}H]AMC were collected and suspended in 0.3 ml of 0.05 M Tris–HCl, pH 7.5, containing 150 mM NaCl. Acetone (4:3 acetone: sample *v*/*v*) was added and samples were mixed and frozen at -80°C for 1 h to fully precipitate protein. Samples were thawed and centrifuged at 2,000×*g* for 15 min and supernatants and pellets were separated. The supernatants containing the protein-free maytansinoid catabolites were evaporated to dryness using an evacuated centrifuge. The residues were dissolved in 0.12 ml of 20% (*v*/*v*) aqueous acetonitrile containing 0.025% (*v*/*v*) trifluoroacetic acid, and the maytansinoid catabolites were separated by HPLC on an analytical C-18 column (Vydac 218TP104, 0.46×25 cm) (6). The effluent was collected in 1 ml fractions and the radioactivity associated with each fraction was determined by mixing each vial with Ultima Gold liquid scintillation cocktail (4 ml) before counting by LSC. The acetone pellet was re-suspended as described above before counting by LSC.

Quantification of Lysine-SMCC-DM1 by LC/MS

The amount of catabolite formed in cells treated with J2898A-SMCC-DM1 was determined by LC/MS. A high resolution mass spectrometry (Q-Exactive, Thermo Scientific) was used with reverse phase column separation utilizing a UHPLC (Dionex). Selected ion monitoring (SIM) data were acquired at 70,000 mass resolution to minimize matrix interference. The peak area ratio of the catabolite ion in the sample *vs.* the molecular ion of the isotope-labeled internal standard was calculated and then translated to the amount of the catabolite based on the linear regression of a standard curve. This value was then normalized to picomoles per million cells according to the original sample amount.

RESULTS

Conjugate Characterization

All [^{3}H]Ab samples had a specific radioactivity in the range of 22.5–48.8 Ci/mmol and had≤1.1% unconjugated tritium label. The ratio of linked [^{3}H]propionamide label per Ab molecule was in the range of 0.28–0.38 mol/mol. The EGFR-targeting [^{3}H]AMC sample (J2898A-SMCC-[^{3}H]DM1) had a specific radioactivity of 0.78 Ci/mmol and contained 2.1% unconjugated tritium label. The ratio of linked maytansinoid molecules per antibody molecule (MAR) for this preparation was 3.06, while that of a non-radiolabeled conjugate used in some experiments was 3.6. See Table I.

Comparison of [^{3}H]J2898A and J2898A-SMCC-[^{3}H] DM1 Processing From FaDu and H292 Tumor Cell Lines

The [^{3}H]Ab and [^{3}H]AMC are expected to enter the cell *via* target-mediated endocytosis and be degraded within lysosomes to component amino acids in a similar manner. In order to confirm this, we labeled the anti-EGFR antibody J2898A with either the *N*-hydroxysuccinimidyl ester of [^{3}H] propionic acid, or with -SMCC-[^{3}H]DM1 and compared the processing of the resulting [^{3}H]J2898A or radiolabeled maytansinoid conjugate by the EGFR-expressing FaDu and H292 cell lines. The time course of processing was monitored and showed a similar increase in radiolabeled small

Table I Study Reagents – All Antibodies [^{3}H]-Propionate-Labeled Except Last

Target	Conjugated Ab	CPM/μL	Specific radioactivity (Ci/mmol)	Concentration (mg/mL)	Unbound [^{3}H] Label	Ratio of [^{3}H]label/Ab (mol/mol)
CD19	[^{3}H]huB4	343,697	26.6	1.47	0.5%	0.33
CD20	[^{3}H]rituximab	451,922	30.4	1.69	0.6%	0.38
CD22	[^{3}H]huBU59	370,927	22.5	1.87	0.5%	0.28
CD37	[^{3}H]K7153A	366,817	28.4	1.47	0.4%	0.36
EGFR	[^{3}H]J2898A	531,371	48.8	1.20	1.1%	0.61
EGFR	J2898A-SMCC-[^{3}H]DM1	29,837	0.78	1.36	2.1%	3.06

molecular weight catabolite, plateauing by about 24 h. Mass balance calculations demonstrated that the total radiolabel present at time zero was accounted for by the sum of all fractions at each sampling point. To compare test articles, we focused on a 22–24 h time point which allows sufficient time for internalization and degradation, but is prior to significant levels of cell death that will be induced by the maytansinoid-loaded reagent. The percentage of target-mediated processing after 22 h was very similar for both samples with 23–31% degradation in FaDu cells and 36–40% degradation in H292 cells (Fig. 2). In addition, the ABC values derived using both methods were similar (~165,000 on both cell lines). This suggests that the approach of using [^{3}H]propionate to label antibody yields comparable results for processing efficiency and metabolism as the previously described procedures for radiolabeled conjugates made using [^{3}H]-labeled maytansinoids (illustrated schematically in Fig. 3).

Identification and Comparison of Catabolite Formation by [^{3}H]J2898A, J2898A-SMCC-[^{3}H]DM1 and J2898A-SMCC-DM1

Catabolite -containing extract from EGFR-expressing Detroit 562 cells treated with [^{3}H]J2898A was analyzed by HPLC using HILIC separation followed by LSC counting of eluted fractions. A single peak was observed and identified as [^{3}H] propionamido-lysine catabolite based on coelution with a synthetic standard (Fig. 4a).

As reported previously for other Ab-SMCC-DM1 conjugates (11,13,14), radiolabeled J2898A-SMCC-[^{3}H]DM1 produced a single catabolite after incubation with FaDu cells (see Fig. 4b). Similarly, H292 cells treated under the same conditions with unlabeled J2898A-SMCC-DM1 also gave one catabolite peak which was identified as lysine-N^{ε}-SMCC-DM1 using HPLC separation *via* C-18 column followed by mass spectral analysis of cell extracts (see Fig. 4c). The cell extracts were spiked with a known amount of isotopically enriched [$^{13}C_6$-$^{15}N_2$] lysine-N^{ε}-SMCC-DM1 internal standard prior to analysis, and quantified using the standard concentration and ratio compared to the sample catabolite peak. The doublet peaks seen in Fig. 4c correspond to the two diastereomers in the thioether linkage of lysine-N^{ε}-SMCC-DM1. When normalized for the differences in the molar ratio of the radiolabel per Ab, the amounts of the [^{3}H] propionamido-lysine and lysine-N^{ε}-SMCC-DM1 catabolite calculated from treatment of the same preparation of H292 cells with [^{3}H]J2898A and J2898A-SMCC-[^{3}H] DM1, respectively, was found to be the same (see Table II).

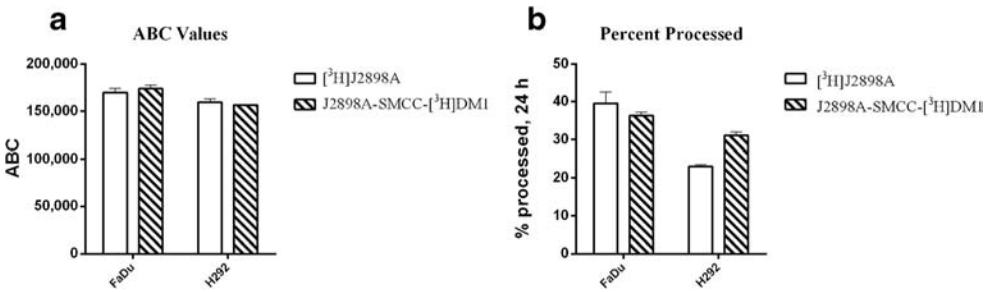

Fig. 2 Comparison of [^{3}H]J2898A and J2898A-SMCC-[^{3}H]DM1 processing by FaDu and H292 cells to yield catabolites of low molecular weight. Cultures of FaDu and H292 tumor cells were exposed to a saturating concentration of [^{3}H]J2898A (*white bars*) or J2898A-SMCC-[^{3}H] DM1 (*striped bars*), washed extensively and incubated at 37°C with 5% CO_2 for 22 h. (**a**) The total sample CPM values were converted to ABC. (**b**) The percent of processed sample, as indicated by soluble [^{3}H] CPM/total sample CPM, is plotted for [^{3}H]J2898A and J2898A-SMCC-[^{3}H]DM1.

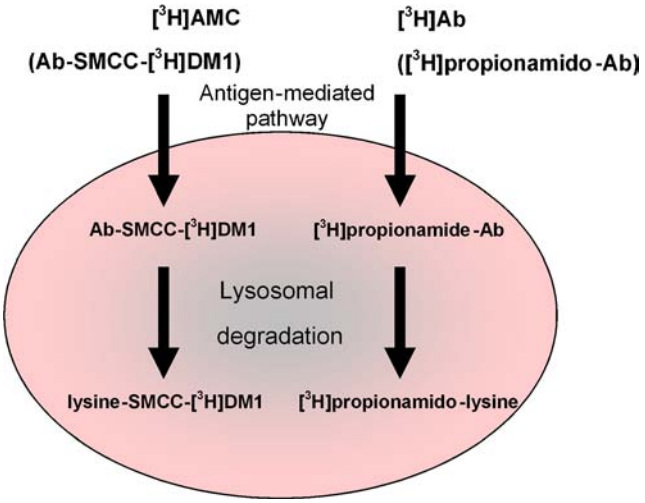

Fig. 3 Model for cellular processing of [^{3}H]AMC and [^{3}H]Ab. [^{3}H]Ab is processed in the same manner as Ab-SMCC-[^{3}H]DM1 conjugate. The radiolabeled conjugate is internalized by antigen-mediated endocytosis, delivered to the lysosomes, and hydrolyzed to [^{3}H]propionamido-lysine. In the case of AMC, the lysosomal derivative is lysine-SMCC-[^{3}H]DM1.

EGFR-Mediated Processing on a Panel of SCCHN Cell Lines

After demonstrating similarity of the extent of processing of [^{3}H]J2898A and J2898A-SMCC-[^{3}H]DM1 by FaDu and H292 cells (see Fig. 2b), we determined the ABC values, percent processing and amount of catabolite produced by a panel of EGFR-expressing cell lines of squamous cell carcinoma of the head and neck (SCCHN) using the [^{3}H]Ab assay. We found EGFR expression, as guided by ABC values, had about at 10-fold range on the 9 of the 10 cell lines tested, with ABC values, from 81,000 to 747,000 ABC (Fig. 5a). One cell line, HSC2, was measured to have over 2 million ABC. The percent of [^{3}H]J2898A degraded (% processed) after the pulse exposure (30 min + wash) averaged about 20% in these cell lines (range from 11 to 28%) (Fig. 5b).

Although the percent processing of [^{3}H]J2898A was nominally similar for all SCCHN cell lines tested, the total amount of degraded antibody varied widely due to the difference in EGFR expression. For example, although HSC2 cells processed [^{3}H]J2898A to the same extent in 22 h as SCC9 cells, the amount of catabolite produced was 45-fold greater due to the antigen expression level difference (see Fig. 5c).

Binding of B-Cell Directed Antibodies and Determination of ABC Values

In order to compare the antigen-mediated processing of antibodies against several B-cell targets, we produced anti-CD37,

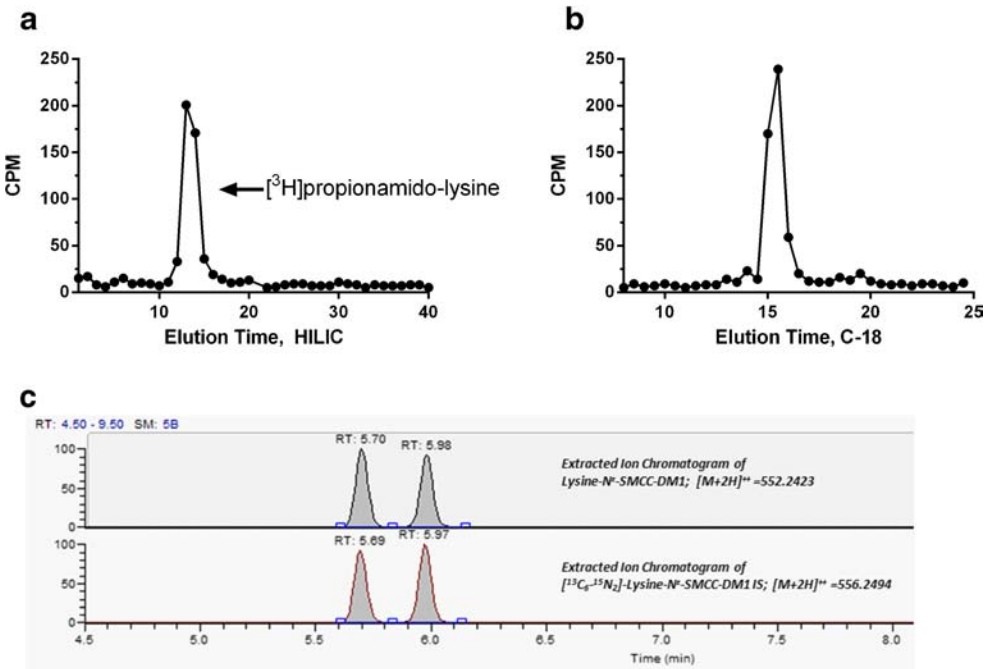

Fig. 4 [^{3}H]Ab, [^{3}H]AMC and AMC *in vitro* catabolite identification by HPLC, LSC and LC/MS. Detroit 562 cells were exposed to [^{3}H]J2898A for 30 min at 37°C, washed extensively, and then, incubated for 22 h at 37°C. Protein-free cell extract (degraded [^{3}H-]J2898A) was analyzed by HILIC column and fractions were counted by LSC. A single catabolite co-eluted with a purified lysine-propionate standard (**a**). FaDu cells were exposed to J2898A-SMCC-[^{3}H]DM1 for 30 min at 37°C, washed extensively and incubated for 22 h at 37°C. Protein-free cell extract (processed conjugate) was analyzed by C-18 and fractions were counted by LSC. A single catabolite was seen (**b**). H292 cells were exposed to non-radiolabeled J2898A-SMCC-DM1 for 30 min at 37°C, washed extensively and incubated for 22 h at 37°C. Cells were extracted with acetone and the internal standard, [$^{13}C_6$-$^{15}N_2$]lysine-N^{ε}-SMCC-DM1, was added to the resulting protein-free cell extract. The extract was analyzed by LC/MS and the SIM chromatogram was plotted for the catabolite (**c**, *top*). The doublet was identified as the two diastereomers of lysine-N^{ε}-SMCC-DM1. The *lower panel* shows the doublet associated with the internal standard (IS) (**c**, *bottom*).

Table II Comparison of Catabolite Formed in H292 Tumor Cells Using LSC or LC/MS Methods

Analysis	Reagent	Catabolite species	Catabolite/ 10^6 cells (pmoles)	Label/Ab	Degraded Ab/ 10^6 cells (normalized to Ab) (pmoles)
C-18 and LSC	[^{3}H]J2898A	[^{3}H]propionamido-lysine	0.162	0.4	0.41
C-18 and MS	J2898A-SMCC-DM1 + internal standard	lysine-SMCC-DM1	1.58	3.6	0.44

anti-CD20, anti-CD22 and anti-CD19 [^{3}H]propionamide-labeled antibodies as described above. We performed pulse-exposure experiments with these antibodies on a panel of NHL cell lines and determined the ABC values for each [^{3}H]Ab/cell line pair. The ABC values obtained from these experiments are shown in Fig. 6a. Among the targets and cell lines tested, ABC values ranged from low values of about 23, 000 (CD19, CD22) to 1,100,000 (CD20 on SU-DHL-4 cells). The values we obtained correlate well with those determined by flow cytometry experiments using phycoerythrin-labeled antibodies as well as published information for CD37, CD19, CD20 and CD22 (14). These results also demonstrate that the binding properties of the antibodies were not affected by conjugation to the radiolabel.

Processing of B-Cell Directed Antibodies

The extent of processing after pulse exposure and 24 h incubation at 37°C of [^{3}H]Ab-treated samples varied from 2 to 43% dependent on the antigen and cell line (see Fig. 6b). The percent processing of the anti-CD37 antibody averaged 12% for the 6 cell lines tested (6% Farage - 16% BJAB). The percent processing

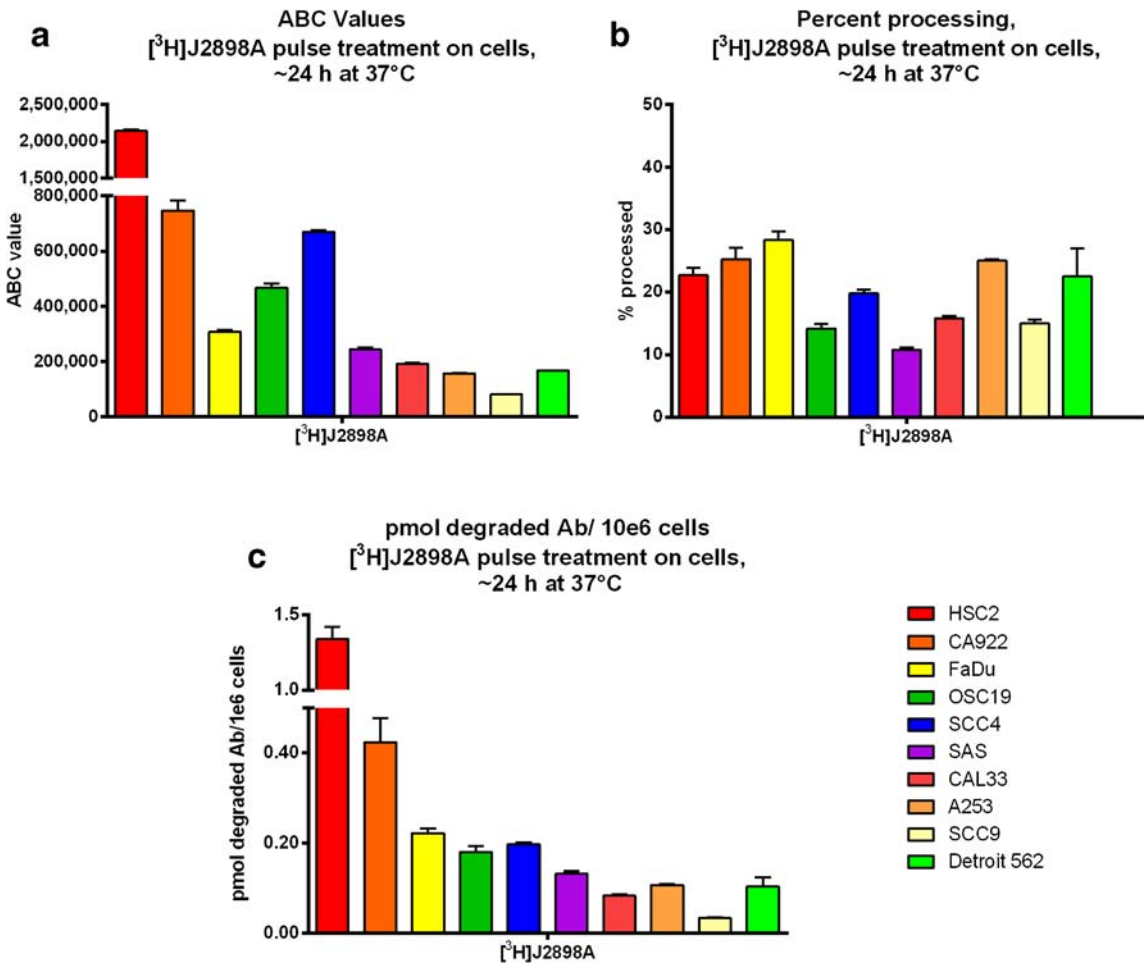

Fig. 5 [^{3}H]J2898A pulse processing on a panel of SCCHN cell lines. After target saturation, thorough washing, 22 h incubation at 37°C with 5% CO_2 and cell harvest, the total sample CPM values were converted to ABC, with values ranging from 81,400–2,150,000 (**a**). The amount of processed [^{3}H]J2898A, defined as the soluble extract [^{3}H] CPM/total sample CPM, is plotted for all cell lines and targets tested. Values range from 11 to 28% (**b**). Picomoles of degraded [^{3}H]J2898A per million cells data are plotted for all cell lines and targets tested. Values range from 0.03 to 1.34 pmole/ 1×10^6 cells (**c**). Variation among replicates is designated with error bars.

of the anti-CD19 antibody averaged about 24% (10% SU-DHL-4 - 43% Ramos). The percent processing of the anti-CD22 antibody averaged 27% (10% SU-DHL-4 - 39% Farage). Lastly, the anti-CD20 antibody rituximab showed the least processing efficiency with less than 5% processing noted on all cell lines tested. Overall, the CD19- and CD22-directed [^{3}H]Abs had the highest extent of processing in 24 h of the targets tested followed by the CD37-directed antibody. As often reported, we found that the CD20-directed antibody rituximab was processed poorly by all cell lines tested (20–22). The variability in percent processing represented by these targets differed somewhat from the EGFR results in Fig. 5. The CD37 and CD20 values were closely matched for all 6 cell lines and CD22 was similar for 5 of the 6, with SU-DHL-4 cells processing at a lower level. However, the variation in processing for the CD19-directed samples was larger than that for the other B-cell targets, with three cell lines showing lower processing (14%) and three cell lines showing more modest processing (33%). We do not know if the differences seen in CD19-mediated processing represent uncharacterized cell line differences (*e.g.*, variability in internalization, trafficking, and/or lysosome degradation) that are not present in the selected set of EGFR, CD37, and CD20 cell-line representatives. It may be that an expanded set of cell lines would help to clarify these differences, or perhaps a more detailed mechanistic study of the processing cascade in two differing cell lines (out of scope here) could identify a responsible factor.

Comparison of Total Catabolite Formation by B-Cell Directed Antibodies

The amount of catabolite produced by the B-cell directed antibodies after pulse exposure and 24 h incubation at 37°C varied depending on the cell line and antibody tested and ranged from 0.01 to 0.13 pmol degraded Ab per million cells. Of the targets tested, the anti-CD37 antibody produced high values for catabolites in 5 of 6 cell lines (see Fig. 6c). Although the percent processing of the anti-CD37 antibody was moderate (6 to 16%), the relatively high antigen expression level on the NHL lines tested resulted in high values for catabolite formation. CD22 and CD19-targeting antibodies produced similar amounts of catabolite as the anti-CD37 antibody, but there was more variation seen between cell lines. Although processing of anti-CD19 and anti-CD22 antibodies reached approximately 40% in some cell lines, the relatively low

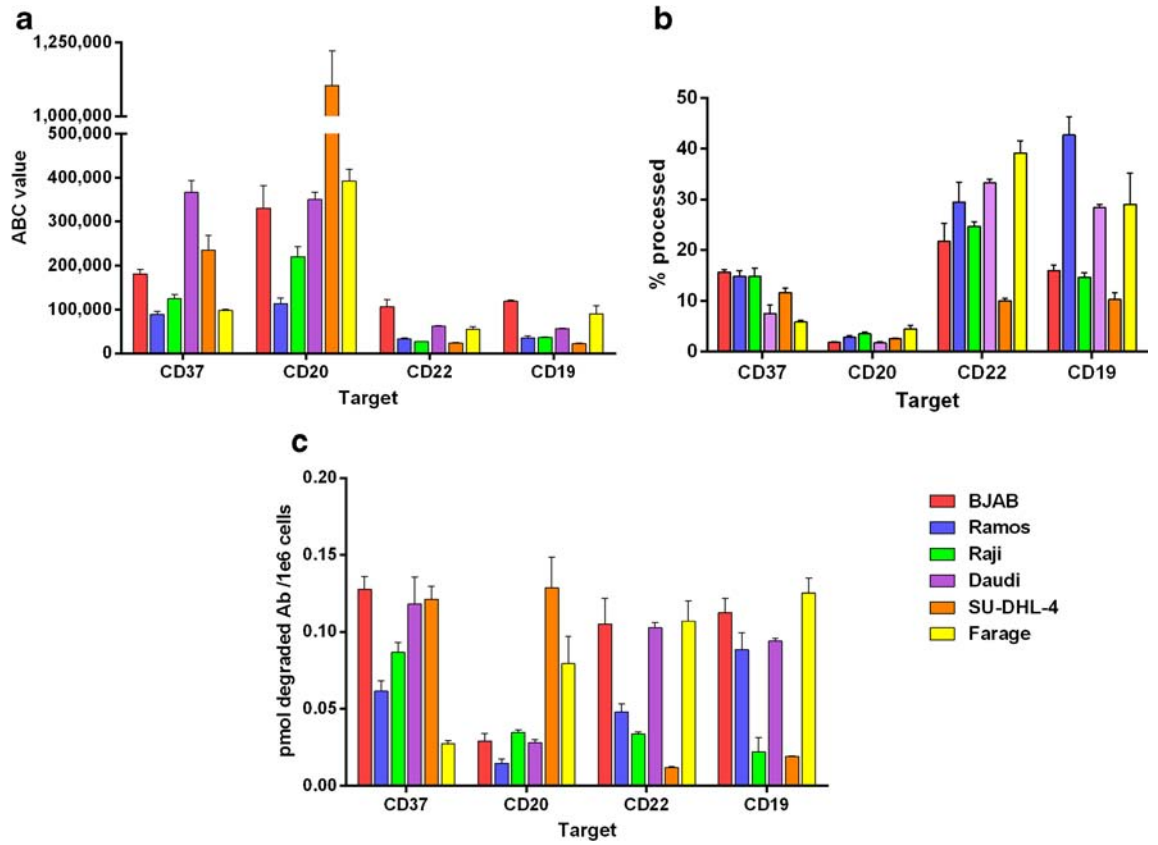

Fig. 6 B-cell targeting [^{3}H]Ab pulse processing on a panel of NHL cell lines. The total sample CPM values were converted to ABC (**a**). The amount of processed [^{3}H]Ab, defined as the soluble extract [^{3}H] CPM /total sample CPM, is plotted for all cell lines and targets tested. Values range from 2 to 43% after 22 h incubation at 37°C with 5% CO_2 (**b**). The picomoles of degraded [^{3}H]Ab per million cells data are plotted for all cell lines and targets tested. Values range from <0.01 to 0.05 pmole/ 1×10^6 cells after 22 h incubation at 37°C with 5% CO_2 (**c**). The average results of multiple independent experiments are shown here (Average of 3 independent experiments run in triplicate, range of $N = 1-8$)

antigen expression level on many of the cell lines often produced a smaller amount of catabolite overall. The CD20-targeting antibody rituximab resulted in≤0.03 pmol degraded Ab per million cells in 4 of 6 cell lines tested. However, [^{3}H]rituximab processing in SU-DHL-4 and Farage, both DLBCL lines, produced high values of catabolite due to the high CD20 expression in these cells.

DISCUSSION

Radiolabeled maytansinoid reagents have provided powerful insight into the mode of action of AMCs as well as enabled comparison of different target antigens for their ability to mediate the essential steps of uptake and catabolism (6,11,23). However, the synthesis of labeled maytansinoid is cumbersome and expensive, limiting the application of this technique. We have therefore developed a convenient [^{3}H]propionamide antibody-labeling technique described here as a simple proxy for measuring relative and total processing levels of antibodies across a variety of antigens and cell lines. We show that data from [^{3}H]propionamide-labeled Abs correlate well with that obtained from the corresponding AMCs. Thus, similar values were obtained for ABC level and the percentage of processing of pulse-labeled cells using the EGFR-targeting J2898A antibody labeled with [^{3}H]-propionate or with [^{3}H]-labeled maytansinoid (DM1). In addition to the cost savings of using an off-the-shelf radiolabeling reagent, we were also able to use 20-fold fewer cells per replicate due to the high specific radioactivity of the [^{3}H] propionamido-antibody, saving time spent culturing and harvesting cells and decreasing sample volume and handling. Further efficiencies were achieved by measurement of the single easily-extractable propionamido-lysine catabolite by total LSC instead of lengthy HPLC analysis.

Using [^{3}H]J2898A we screened 10 SCCHN cell lines and found that, despite wide variation in the amount of EGFR expression, the extent of EGFR-mediated processing in ~24 h was very similar on all cell lines tested (range 10 to 25%, average 20%). The ABC value, however, was much more variable (81,000 to 2,100,000, a 26-fold range). The majority of cell lines tested (6 of 10) had ABC values around 300,000 and yielded ~0.2 picomoles of degraded J2898A antibody per million cells based on ~20% processing. For the chosen SCCHN lines expressing EGFR, since the extent of processing over ~24 h did not show much variation, the primary determinant for the total amount of antibody degraded in 24 h was the more variable ABC value.

To further exemplify the utility of the [^{3}H]Ab labeling method, we examined antibodies to various B-cell targets, CD19, CD20, CD22 and CD37, on a range of NHL cell lines and compared the results of antigen expression and pulse-exposure processing. We found different processing for the 4 targets analyzed on each of the 6 cell lines. For CD37 and CD20, this percent processing was largely consistent across the cell lines tested. This observation is consistent with an equivalent percent of EGFR-mediated processing by a panel of SCCHN cell lines assessed with [^{3}H]J2898A, suggesting that the processing rate *in vitro* is driven more by the properties of these individual targets, than by the cell lines. However, for CD22 and CD19, processing was more variable. It is possible that uncharacterized differences in the cell lines studied here, such as internalization, trafficking, or lysosomal degradation, are responsible. Further studies to probe these differences can include an expansion of the cell lines tested for each target, to see how the variability holds across larger data sets, as well as an investigation into the kinetics and mechanism of internalization and catabolite formation that could identify differences among cell lines.

Among the B-cell targets explored, the processing rate of CD20 was consistently low, as reported previously. However, when comparing the amount of total catabolite, as measured by degraded antibody, CD20 ranked highest on the DLBCL cell line SU-DHL-4. This demonstrates that high target expression (that is, high ABC level) can compensate for a modest extent of processing. Conversely, a similar level of catabolite could also be generated when a cell line with moderate expression processed [^{3}H]Ab to a greater extent over 24 h, as seen in the case of Farage cells treated with [^{3}H]propionamide-labeled anti-CD19 or anti-CD22. Only by accounting for both the target expression level and the efficiency of intracellular processing of antibody measured after 24 h, can the utility of a given target be judged for its potential as an ADC target. Indeed, when these three targets were studied as calicheamicin ADCs, although the anti-CD20 conjugate caused significant growth inhibition of B-cell lymphoid cell lines, it was less effective than the conjugates of anti-CD22 or anti-CD19 Abs (24).

The *in vitro* sensitivity of cancer cells to ADCs is governed by many factors including antigen density and the rate and extent of antigen-mediated degradation. While data obtained from studies run with [^{3}H]propionamide-labeled antibodies can readily give quantitative measurements of these two elements, additional factors must be considered in order to predict and understand ADC activity. These include the sensitivity of a particular cell line to the maytansinoid effector and any anti-proliferative activity of the antibody component of the ADC (14). In particular, if inherent antibody activity is sought for a particular target, separate biological assays should be considered in order to select candidates. Although the 24 h pulse processing data for the targets studied here appear to correlate well across different cell lines, as a practical consideration it is prudent to assess processing in multiple cell lines for the target of interest, rather than rely on measurements on a single cell line. For example, considering the processing of

the anti-CD22 antibody (Fig. 5b), the SU-DHL-4 cell line has a much lower extent of processing in 24 h than the other 5 cell lines and may thus be atypical for this property.

CONCLUSION

The [^{3}H]propionamide-Ab assay described here offers a robust, sensitive and inexpensive method to simultaneously analyze antigen expression, target-mediated lysosomal processing and catabolite formation. A direct comparison of Ab-SMCC-[^{3}H]DM1 alongside [^{3}H]propionamide-Ab, suggests that a similar path of antigen-mediated uptake and lysosomal degradation was followed to produce a single catabolite: lysine-SMCC-DM1 and propionamido-lysine, respectively, as a consequence of complete proteolysis of the antibody in the lysosome to its constituent amino acid residues. Since the *N*-succinimidyl[^{3}H]propionate reagent is commercially available, and of high specific radioactivity, one can easily prepare radiolabeled antibodies and execute assays to quickly obtain information relevant to assessing a target, and antibodies to a given target, for utility as an ADC candidate. The [^{3}H]Ab method results in strong and consistent signal on even low antigen-expressing cell lines and also enables much smaller sample sizes making it faster and easier to screen desired targets and indications.

Exploration of cell lines from multiple indications using the [^{3}H]Ab assay has generated useful data relating deliverable catabolite levels. The information acquired from these assays helps gauge how candidate ADCs would perform to a given target expressed on a variety of representative cancer cell lines.

ACKNOWLEDGMENTS AND DISCLOSURES

We thank our colleagues Min Li, Yong Yi and Anna Skaletskaya for their contributions to the work presented here and Dr. Thomas Keating for his thorough review of the manuscript.

REFERENCES

1. Lambert JM. Drug-conjugated antibodies for the treatment of cancer. Br J Clin Pharmacol. 2013;76(2):248–62.
2. Ribrag V, Dupuis J, Tilly H, Morschhauser F, Laine F, Houot R, *et al.* A dose-escalation study of SAR3419, an anti-CD19 antibody maytansinoid conjugate, administered by intravenous infusion once weekly in patients with relapsed/refractory B-cell non-Hodgkin lymphoma. Clin Cancer Res Off J Am Assoc Cancer Res. 2014;20(1):213–20.
3. Chari RV, Miller ML, Widdison WC. Antibody-drug conjugates: an emerging concept in cancer therapy. Angew Chem. 2014;53(15):3796–827.
4. Whiteman KR, Johnson HA, Mayo MF, Audette CA, Carrigan CN, LaBelle A, *et al.* Lorvotuzumab mertansine, a CD56-targeting antibody-drug conjugate with potent antitumor activity against small cell lung cancer in human xenograft models. mAbs. 2014;6(2):556–66.
5. Raufi A, Ebrahim AS, Al-Katib A. Targeting CD19 in B-cell lymphoma: emerging role of SAR3419. Cancer Manag Res. 2013;5:225–33.
6. Erickson HK, Park PU, Widdison WC, Kovtun YV, Garrett LM, Hoffman K, *et al.* Antibody-maytansinoid conjugates are activated in targeted cancer cells by lysosomal degradation and linker-dependent intracellular processing. Cancer Res. 2006;66(8):4426–33.
7. Oroudjev E, Lopus M, Wilson L, Audette C, Provenzano C, Erickson H, *et al.* Maytansinoid-antibody conjugates induce mitotic arrest by suppressing microtubule dynamic instability. Mol Cancer Ther. 2010;9(10):2700–13.
8. Erickson HK, Lewis Phillips GD, Leipold DD, Provenzano CA, Mai E, Johnson HA, *et al.* The effect of different linkers on target cell catabolism and pharmacokinetics/pharmacodynamics of trastuzumab maytansinoid conjugates. Mol Cancer Ther. 2012;11(5):1133–42.
9. Kovtun YV, Audette CA, Mayo MF, Jones GE, Doherty H, Maloney EK, *et al.* Antibody-maytansinoid conjugates designed to bypass multidrug resistance. Cancer Res. 2010;70(6):2528–37.
10. Blanc V, Bousseau A, Caron A, Carrez C, Lutz RJ, Lambert JM. SAR3419: an anti-CD19-Maytansinoid Immunoconjugate for the treatment of B-cell malignancies. Clin Cancer Res Off J Am Assoc Cancer Res. 2011;17(20):6448–58.
11. Erickson HK, Widdison WC, Mayo MF, Whiteman K, Audette C, Wilhelm SD, *et al.* Tumor delivery and in vivo processing of disulfide-linked and thioether-linked antibody-maytansinoid conjugates. Bioconjug Chem. 2010;21(1):84–92.
12. Sun X, Widdison W, Mayo M, Wilhelm S, Leece B, Chari R, *et al.* Design of antibody-maytansinoid conjugates allows for efficient detoxification via liver metabolism. Bioconjug Chem. 2011;22(4):728–35.
13. Shen BQ, Bumbaca D, Saad O, Yue Q, Pastuskovas CV, Khojasteh SC, *et al.* Catabolic fate and pharmacokinetic characterization of trastuzumab emtansine (T-DM1): an emphasis on preclinical and clinical catabolism. Curr Drug Metab. 2012;13(7):901–10.
14. Deckert J, Park PU, Chicklas S, Yi Y, Li M, Lai KC, *et al.* A novel anti-CD37 antibody-drug conjugate with multiple anti-tumor mechanisms for the treatment of B-cell malignancies. Blood. 2013;122(20):3500–10.
15. Burke P, Schooler K, Wiley HS. Regulation of epidermal growth factor receptor signaling by endocytosis and intracellular trafficking. Mol Biol Cell. 2001;12(6):1897–910.
16. Elia G. Biotinylation reagents for the study of cell surface proteins. Proteomics. 2008;8(19):4012–24.
17. Widdison WC, Wilhelm SD, Cavanagh EE, Whiteman KR, Leece BA, Kovtun Y, *et al.* Semisynthetic maytansine analogues for the targeted treatment of cancer. J Med Chem. 2006;49(14):4392–408.
18. Asai MK, Izawa M (1981) Inventors demethyl maytansinoids USA patent 4307016.
19. Sawada T, Kato Y, Kobayashi H, Hashimoto Y, Watanabe T, Sugiyama Y, *et al.* A fluorescent probe and a photoaffinity labeling reagent to study the binding site of maytansine and rhizoxin on tubulin. Bioconjug Chem. 1993;4(4):284–9.
20. Sapra P, Allen TM. Internalizing antibodies are necessary for improved therapeutic efficacy of antibody-targeted liposomal drugs. Cancer Res. 2002;62(24):7190–4.
21. Press OW, Farr AG, Borroz KI, Anderson SK, Martin PJ. Endocytosis and degradation of monoclonal antibodies targeting human B-cell malignancies. Cancer Res. 1989;49(17):4906–12.
22. Vangeepuram N, Ong GL, Mattes MJ. Processing of antibodies bound to B-cell lymphomas and lymphoblastoid cell lines. Cancer. 1997;80(12 Suppl):2425–30.

23. Erickson HK, Lambert JM. ADME of antibody-maytansinoid conjugates. AAPS J. 2012;14(4):799–805.
24. DiJoseph J, Armellino DC, Dougher MM, Kunz A, Boghaert ER, Hamann PR, et al. Antibody-targeted chemotherapy with immunoconjugates of calicheamicin: differential anti-tumor activity of conjugated calicheamicin targeted to B-cell lymphoma via B-cell lineage specific molecules CD19, CD20 and CD22. Blood. 2004; ASH Annual Meeting Abstracts(104).